Nonlinear dielectric behavior in three-component ferroelectric superlattices

A. Sarkar, R. Ranjith, and S. B. Krupanidhi

Citation: Journal of Applied Physics **102**, 024108 (2007); doi: 10.1063/1.2753574
View online: http://dx.doi.org/10.1063/1.2753574
View Table of Contents: http://scitation.aip.org/content/aip/journal/jap/102/2?ver=pdfcov
Published by the AIP Publishing

Nonlinear dielectric behavior in three-component ferroelectric superlattices

A. Sarkar, R. Ranjith, and S. B. Krupanidhi[a)]
Materials Research Center, Indian Institute of Science, Bangalore-560 012, India

(Received 20 April 2007; accepted 29 May 2007; published online 20 July 2007)

Three-component ferroelectric superlattices consisting of alternating layers of $SrTiO_3$, $BaTiO_3$, and $CaTiO_3$ (SBC) with variable interlayer thickness were fabricated on $Pt(111)/TiO_2/SiO_2/Si$ (100) substrates by pulsed laser deposition. The presence of satellite reflections in x-ray-diffraction analysis and a periodic concentration of Sr, Ba, and Ca throughout the film in depth profile of secondary ion mass spectrometry analysis confirm the fabrication of superlattice structures. The P_r (remnant polarization) and P_s (saturation polarization) of SBC superlattice with 16.4-nm individual layer thickness (SBC16.4) were found to be around 4.96 and 34 $\mu C/cm^2$, respectively. The dependence of polarization on individual layer thickness and lattice strain were studied in order to investigate the size dependence of the dielectric properties. The dielectric constant of these superlattices was found to be much higher than the individual component layers present in the superlattice configuration. The relatively higher tunability ($\sim$55%) obtained around 300 K indicates that the superlattice is a potential electrically tunable material for microwave applications at room temperature. The enhanced dielectric properties were thus discussed in terms of the interfacial strain driven polar region due to high lattice mismatch and electrostatic coupling due to polarization mismatch between individual layers. © *2007 American Institute of Physics*.
[DOI: 10.1063/1.2753574]

I. INTRODUCTION

Three-component perovskite superlattices have gained interest in the recent years due to their superior properties in terms of enhancement of polarization. They are known for the symmetry breaking along a crystallographic direction and effectively giving rise to polar interfaces and hence effectively enhance the polarization.[1–3] Influence of interfacial strain in the polarization enhancement has been reported both theoretically and experimentally elsewhere.[1,2,4–6] Apart from its enhancement in the properties, it is also possible to design the superlattice with new properties entirely different from the property of any of the parent members present.[7–9] Various experimental and theoretical models have been studied extensively explaining the role of intrinsic coupling, effect of interfacial coupling and the interfacial strain on ferroelectric superlattices.[10–14] The role of depolarizing field in the polarization reduction in ultrathin films was shown and an electrostatic model generalized for thin films was introduced.[15–17] A thermodynamic model to understand the interlayer coupling in multilayer ferroelectric heterostructures was developed recently.[18–20] The wide range of applications of ferroelectric oxides which include ferroelectric memories, microelectromechanical system (MEMS) devices, voltage tunable microwave devices, etc., requires a precise combination of properties of individual layers. Extensive research has been carried out to obtain large dielectric constant and non-linear dielectric properties due to their fundamental importance in electrically tunable microwave devices. The voltage dependence of the dielectric constant is one of the most sought behaviors for a variety of applications. This feature is used to produce voltage-tunable microwave devices such as tunable filters, phase shifters, and resonators.[21,22] It is desirable to fabricate thin films, which have maximum tunability with minimum dielectric loss. Several promising perovskite ABO_3 materials have been reported but it has been found that high tunability generally accompanied a high loss. The three-component perovskite systems are known more for their strain induced enhancement of their physical properties than that of the individual constituent of the superlattice structures. Three-component $SrTiO_3/BaTiO_3/CaTiO_3$ (SBC) systems have been studied both theoretically and experimentally on epitaxially grown thin films[1,2,5] and are known to be potential systems for high polarization devices. In any of the ferroelectric superlattice systems the interfaces present and the size of the individual layers play a crucial role in deciding upon the final properties of the system. In this study a highly oriented superlattice structure of SBC with individual layer thickness ranging from 4 to 40 nm were fabricated on $Pt(111)/TiO_2/SiO_2/Si$ (100) substrates through pulsed laser ablation technique. It could be noted that it becomes critical to accurately maintain the periodicity at small individual layer thicknesses (less than 29 nm) for polycrystalline superlattices, which may be due to the interfacial roughness and lack of inconsistency in the deposited layer thickness.[23] The strain in these structures can result in substantial polarization enhancement. However, there is a limit on the size of individual layer thickness and above a certain thickness the strain in the layers relaxes to their native lattice constants. We study the artificial enhancement of physical properties in these superlattice structures and obtain a large dielectric constant and non-linear dielectric properties. The experimental realization of the polarization related properties and their dimensional range in which the overall polarization behavior

[a)]Author to whom correspondence should be addressed; electronic mail: sbk@mrc.iisc.ernet.in

of the system dominates are investigated. We also consider the electrostatic charge, which can largely determine the polarization and structural properties in these systems with materials having different susceptibilities, or a polarization mismatch, and investigate their interfacial behavior. The effect of individual layer thickness on tunability of SBC superlattice for tunable dielectric application is addressed.

II. EXPERIMENTAL PROCEDURE

SBC ferroelectric superlattices were fabricated by a multitarget-pulsed laser deposition technique. A 248-nm KrF excimer laser operated at 3 Hz was alternately focused onto the stoichiometric ceramic targets of ST ($SrTiO_3$), BT ($BaTiO_3$), and CT ($CaTiO_3$) with an energy fluence of 3 J/cm^2. SBC with 4 nm (SBC4), 10 nm (SBC10), 16.4 nm (SBC16.4), 20 nm (SBC20), 24.8 nm (SBC24), and 40 nm (SBC40) individual layer thickness were deposited on $Pt(111)/TiO_2/SiO_2/Si$ (100) substrates at 700 °C and 20 mTorr of ambient oxygen. The superlattices of these selected compositions were deposited one over another *in situ* without breaking the vacuum and without any delay introduced between deposition of successive layers such that a sharp interface is maintained between each layer. The total thicknesses of all the films were about 600 nm. The thickness of the individual layers and the superlattices were optimized using a cross-sectional scanning electron microscope. The crystallinity and the superlattice behavior of these films were characterized by a Scintag powder x-ray diffractometer using a Fe $K\alpha$ source of $\lambda = 1.937$ Å. The sharpness of the interface and the composition gradient observed in the interface were studied using a secondary ion mass spectrometer (Cameca 4*f*). The structures were characterized in the metal-insulator-metal (MIM) configuration and the electrical studies were carried out by keeping the electric field perpendicular to the interfaces present. The top electrodes were annealed at 325 °C for 20 min for the adhesion of the same to the film. The capacitance-voltage (*C-V*) and dielectric studies were performed with an Agilent Technologies 4294A impedance analyzer (4294A) from 100 Hz to 1 MHz. The polarization hysteresis measurements (*P-E*) were carried out using a 3.1.1 Radiant Technologies precision workstation.

III. RESULTS AND DISCUSSION

A. X-ray diffraction and SIMS analysis

Figure 1 shows the x-ray-diffraction pattern of a three-component multilayered heterostructure system with 10-nm individual layer thickness (SBC10 hereafter). The diffraction pattern indicated a preferred orientation of the grains in the (110) direction. The presence of superlattice reflections adjacent to the main peak indicated that the films were heterostructurally coherent with sharp interfaces. The satellite peaks are known to be symmetrically distributed around the main peak from the theoretical calculations of one-dimensional superlattices. The asymmetry in the intensity has been attributed to the fluctuation in the periodicity across the sample. Moreover, the second-order term in the strain corresponding to the interfaces plays a major role in giving rise to an asymmetry in the intensity distribution of satellite peaks in the static phonon model proposed for the one-dimensional superlattices in semiconductor structures.[24] The periodicities of the repeating units (one unit is defined as a trilayer of ST-BT-CT) calculated[25] from the superlattice peak positions matched well with the thickness calibration performed using a scanning electron microscope.

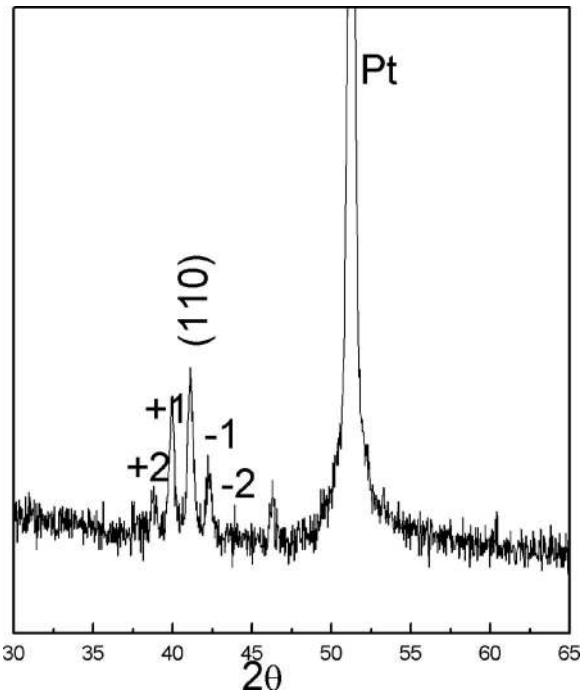

FIG. 1. The XRD pattern of a ST(10 nm)/BT(10 nm)/CT(10 nm) superlattice (SBC10) (Fe $K\alpha$, $\lambda = 1.935$ Å).

Figure 2 shows the depth profile conducted by SIMS analysis of a SBC10 superlattice with individual layer thickness of 10-nm film. Depth profile of Sr, Ba, and Ca shows a clear picture of periodic concentration throughout the film. The periodic modulation of the Sr, Ba, and Ca content through the 20 periods of superlattice is clearly observed. The thickness of Sr, Ba, and Ca layers approximately derived from the full width at half maximum (FWHM) values of the

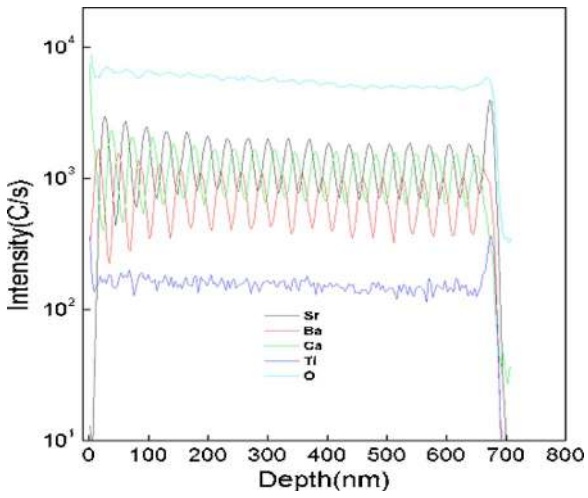

FIG. 2. SIMS based depth profile of a ST(10 nm)/BT(10 nm)/CT(10 nm) superlattice (SBC10).

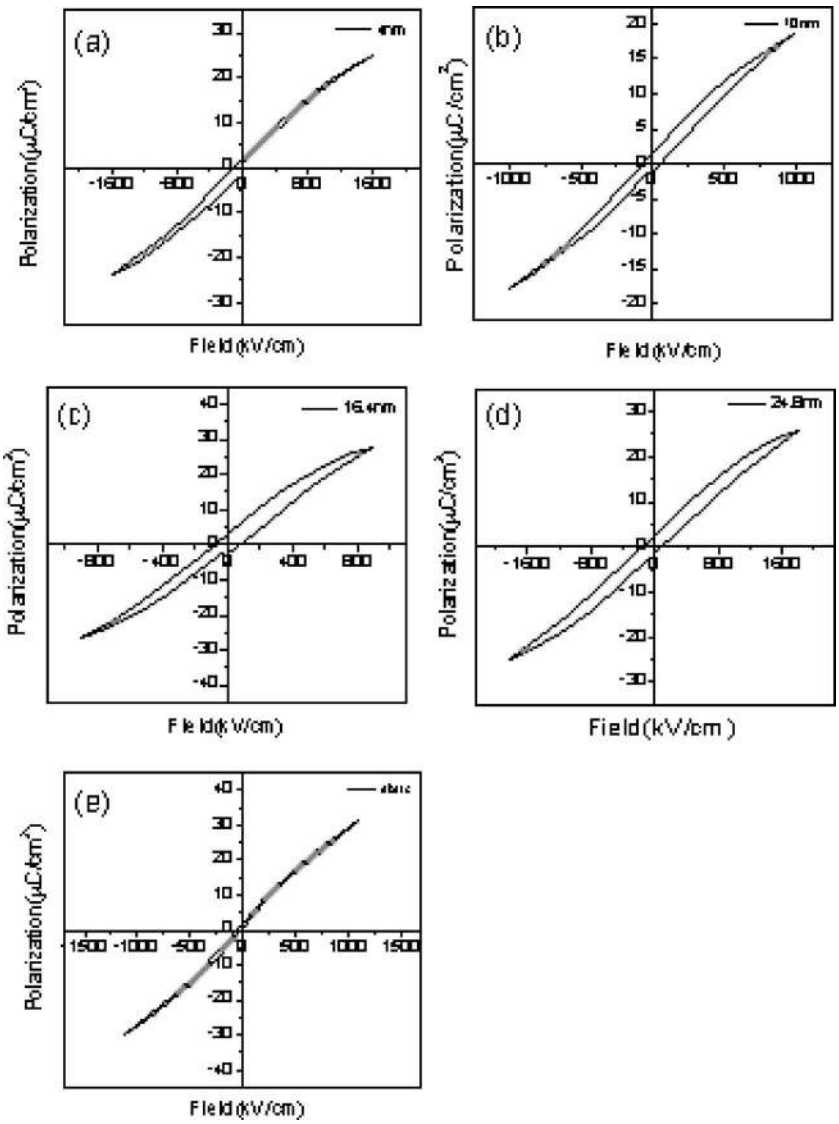

FIG. 3. Polarization hysteresis curves of (a) ST (4 nm)/BT (4 nm)/CT (4 nm), (b) ST (10 nm)/BT (10 nm)/CT (10 nm), (c) ST (16.4 nm)/BT (16.4 nm)/CT (16.4 nm), (d) ST (24.8 nm)/BT (24.8 nm)/CT (24.8 nm), (e) ST (10 nm)/$Ba_{0.8}Sr_{0.2}TiO_3$ (10 nm)/CT (10 nm).

SIMS signal is 10 nm. Results show that the thickness of the layers is kept constant throughout the structure. The abruptness at the interface between the layers was about a few nanometers. Remarkably, sharp transitions at the layer interfaces are observed for the Sr, Ba, and Ca signals. This is indicative of insignificant sample roughness of the ST, BT, or CT surface. The interfaces between individual layers were found to be sharp, which indicates the possible presence of some lattice strain at the interfaces.

B. Hysteresis (*P-E*) measurements

The ferroelectric properties of the superlattice were confirmed by (*P-E*) hysteresis loop measurement at room temperature. Figures 3(a)–3(d) show the polarization hysteresis curve of SBC superlattice with different individual layer thickness at room temperature. The remnant polarization (P_r) and the saturation polarization (P_s) of SBC superlattice with 16.4-nm individual layer thickness (SBC16), found to be around 4.96 and 34 $\mu C/cm^2$, respectively, shows the maximum values for the fabricated structures. The loops were found to be much slimmer than that of the single layer composition, which may be due to the strain field present at the interfaces of the layers. The various intrinsic and extrinsic factors that affect the polarization behavior of any FE thin-film structure are (i) the FE domains and the dipolar interactions, (ii) the depolarizing field, (iii) the electrode effects, and (iv) the other free charges due to defects, misfit dislocations, etc., in the system. The field generated at the interface due to the difference in polarization at the interface could also play a crucial role in stabilizing the ground state of heterostructure systems. All these factors described have their own length scale over which they dominate.[26–28] In the case of these superlattices the interfacial strain associated with them gives rise to a strained polar region acting as a domain. These strained regions arising due to broken symmetry and their chemical heterogeneity are known to play a key role in the polarization enhancement in these superlattices.[2,5] In the case of SBC, there are two active ferroelectric (FE)–paraelectric (PE) interfaces: (i) the BT-ST interface and (ii) the CT-BT interface. The lattice mismatch present in between the ST and BT unit cells is ~2.31% and the CT-BT interface is ~2.48%. Sustainability of strains of this magnitude is expected to increase the polarization in superlattice geometry. Further, CT and BT unit cells tend to

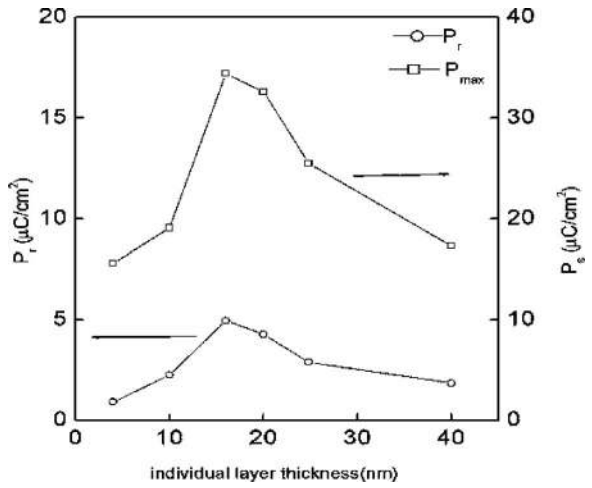

FIG. 4. P_r and P_s (saturation polarization) values of SBC superlattice as a function of individual layer thickness from $E=\pm 1000$ kV/cm.

remain more polar when assembled into thick layers and their presence induces substantial polarization in these superlattices.

The constituent layer thickness dependence on the enhancement of polarization is shown in Fig. 4. P_r and P_s values of SBC superlattice with different individual layer thickness from $E=\pm 1000$ kV/cm loops are plotted. The figure shows a clear thickness dependent polarization behavior of the superlattices. At an individual layer thickness of 4 nm, the system exhibited a slim hysteresis loop with a saturation (P_s) polarization of 15 $\mu C/cm^2$. On increasing interlayer thickness, the saturation (P_s) and remnant (P_r) polarization increases gradually, tends to reach a maximum at a certain thickness, followed by a reduction. This could be due to the partial strain relaxation occurring above a certain layer thickness and thus the polarization decreases. The strain introduced at the interface is much higher at lower dimensions and as we increase the thickness of the individual layers, they relax their structures and behave as individual materials put together. Strain enhancement of the polarization and interfacial effects were clarified when $Ba_{0.8}Sr_{0.2}TiO_3$ (BST) layers instead of BT layers were interleaved between identical ST and CT layers. Figure 3(e) shows the *P-E* curve of ST, BST, CT three-component superlattice (SBSTC) with individual thickness of 10 nm (periodicity 30 nm, total thickness 600 nm) and grown under identical conditions. A very low P_r value of 1 $\mu C/cm^2$, less than SBC10 [Fig. 3(b)] and even SBC4 [Fig. 3(a)] is clearly observed which suggests that the BT-CT interface is more strained and effectively more polar than the BST-CT interface. The lattice mismatch between BST-CT (~2.06%) is less than BT-CT (~2.48%) and hence the lattice strain is lower in that interface. Moreover, BT unit cells are more polar than BST unit cells and tend to remain more polar when assembled into thick layers.

The gradual increase of polarization with decrease of interlayer thickness in these systems may be possible due to the dominance of long-range interaction.[10,12] At lower interlayer thicknesses, the long-range interaction dominates with an intrinsic coupling between the lattices of the heterostructure present and effectively contributes to the ferroelectric characteristics of the system. With further decrease of the interlayer thickness, the contribution of the size effect to the heterostructure begins to dominate, exhibiting a competition between the size effect and long-range coupling interaction. Thus at a finite thickness, the polarization reaches a maximum, and then decreases due to the dominance of the size effect. On increase of the individual layer thickness, the dimension exceeds the critical size over which the long-range interaction among the dipoles are weak and the interfacial coupling dominates over the effective property of the system. In our present work the existence of the long-range interaction could account for the interlayer thicknesses of 4–24 nm, which is within the range of the domination of long-range interaction of dipoles.

It is also important to consider the electrostatic charge, which can largely determine the polarization and structural properties in these systems with materials having different susceptibilities, or a polarization mismatch. The FE heterostructures can be understood by the model based on the thermodynamic free energy of a heterostructure including the electrostatic interactions. The total free-energy density of a multilayer consisting of sets of alternate ferroelectric (FE) and incipient ferroelectric (PE) layers with short circuit conditions and incorporating the potential energies of the internal fields is given as[18–20]

$$F = (1-\alpha)F_{\mathrm{FE}}(P_{\mathrm{FE}}) + \alpha F_{\mathrm{PE}}(P_{\mathrm{PE}}) + \frac{1}{2}\alpha(1-\alpha)\frac{1}{\varepsilon_o}(P_{\mathrm{FE}}-P_{\mathrm{PE}})^2 + \frac{F_s}{h},$$

where $\alpha = t_{\mathrm{FE}}/(t_{\mathrm{FE}}+t_{\mathrm{PE}})$ is the relative thickness of the layers, P_{FE} and P_{PE} are the respective polarization of the FE and PE layer normal to the interlayer interface, and E is an applied electric field parallel to the direction of polarization. F_s/h is the interface energy and can be neglected over very small length scales. The third term on the right-hand side expresses the electrostatic coupling between the layers. F_{FE} (P_{FE}) and F_{PE} (P_{PE}) are the uncoupled free energies of the layers.

The polarizations in the coupled layer can be obtained using the energy minimum conditions at the equilibrium. A mismatch in the polarizations between the layers gives rise to depolarizing field in the both layers. These internal fields in the layers can play a crucial role depending on the values of the polarization of the individual layers. The depolarization field in the layer with lower polarization enhances the polarization, whereas the depolarization field in the layer with high polarization is opposite to the applied field direction and effectively opposes polarization. This internal field has been observed to play a crucial role in deciding the stability of the interlayer.

The major conclusions of the model are as follows: (i) an extremely high dielectric response can be achieved by varying the volume fraction of the layers; (ii) it is possible to induce as much polarization even in the paraelectric (PE) layer by means of having a FE and PE bilayer; and (iii) high tunability could be achieved in the bilayers and superlattices by means of transfer of strain from one layer to the other and by inducing polarization even from FE to PE layer. Thus in the case of a single layer thin film the internal depolarizing

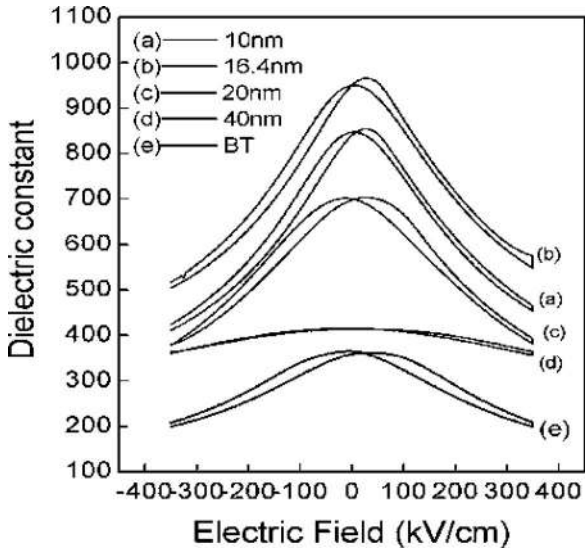

FIG. 5. Room-temperature dielectric constant–electric-field characteristics of SBC superlattice with different individual layer thickness at 1 MHz.

fields can be screened by the electrodes to some extent, but in the case of superlattices there are many active interfaces and there could be ineffective extrinsic screening and hence an increase of the random field inside the heterostructure.[29] The electrostatic coupling depends also on the initial polarization difference and polarizibilty of the constituent layers. Since BT unit cells are more polar than BST unit cells when assembled into thick layers, their presence induces more substantial polarization in the ST and CT incipient ferroelectric (PE) layers than the BST layers. This results in a uniform polarization along the whole superlattice, thereby minimizing the electrostatic energy associated with the buildup of polarization charge at the interface. Second, the initial polarization differences between BST-ST and BST-CT layers are smaller than BT-ST and BT-CT layers, respectively, resulting in less electrostatic coupling effect in SBSTC than in the SBC10 sample. Hence a collective effect of the strain at the interface, enhanced chemical heterogeneity across the film, and the electrostatic coupling effect due to the polarization mismatch could play a collective role in enhancing the property of a given superlattice thin film. Though strain relaxation is more favorable in these polycrystalline systems, the films were found to be highly oriented with the columnar growth structure observed in cross-sectional scanning electron microscope. The observation of a columnar growth of the whole structure indicates a sharp interface between the individual layers and also the absence of any grain boundary perpendicular to the applied field. A very low interfacial average roughness of a few nanometers found between individual layers from SIMS analysis indicates the possible presence of lattice strain present at the interfaces.

C. Capacitance-voltage (*C-V*) measurements

The room-temperature dielectric constant–voltage characteristics obtained from *C-V* characteristics of SBC superlattice structures with different periodicities at 1 MHz are shown in Fig. 5. The magnitudes of the room-temperature dielectric constants in the superlattice structures were found to be remarkably high compared to the values observed for the thin films of individual components with equal total thickness. The *C-V* vs periodicity curves exhibit a clear thickness dependence similar to the corresponding polarization curves, i.e., on decreasing interlayer thickness, the dielectric constant increases gradually and reaches one maximum at a certain thickness. High nonlinear dielectric response as a function of electric field and a butterfly loop behavior commonly observed in normal ferroelectric compositions establishes the ferroelectric nature of the superlattices.[30] The imaginary part of the dielectric constant followed the same trend showed by the real part and was found to be about 10 for all the structures at zero fields. The variation in capacitance with respect to the applied field is measured in terms of tunability and is generally a measure used to characterize the non-linear behavior of a given FE material. The tunability of superlattices was calculated using equation[31]

$$\text{tunability} = \frac{C[\varepsilon](T,0) - C[\varepsilon](T,E)}{C[\varepsilon](T,0)} \times 100\% \ldots ,$$

where $C[\varepsilon]\ (T,0)$ is either the capacitance or dielectric permittivity at a given temperature and zero field, $C[\varepsilon](T,E)$ is the capacitance or dielectric permittivity at the same temperature and at the maximum field. Tunability and *C-V* measurements show that the superlattices exhibited a superior property than that of single layer $BaTiO_3$ thin films and also from their solid solution with $SrTiO_3$. A tunability of 55% was achieved in the case of a superlattice sample with individual layer thickness of 16 nm. It is also worth noting that the tunability appears to be more improved with decreasing thickness of the superlattice individual layer.

The enhancement in the tunability is attributed to the interfacial strain due to lattice mismatch. The strain introduced at the interface is much higher at lower dimensions and as we increase the thickness of the individual layers, they relax their structures and behave as individual materials put together. Hence on higher periodicities, they show a reduced polarization behavior and are effectively seen in the reduction of room-temperature dielectric constants at 1 MHz. The tunability and loss tangent ($\tan\delta$) are important in determining the utility of the material for tunable dielectrics. A figure of merit (FOM) used to evaluate the materials property for tunable devices is given by

$$\text{FOM} = \frac{C[\varepsilon](T,0) - C[\varepsilon](T,E)}{C[\varepsilon](T,0)} X \frac{1}{\tan(\delta)_{\max}}.$$

Figure 6 shows the FOM of the superlattice films with different individual layer thicknesses as a function of applied electric field up to 350 kV/cm. The FOM values at 350 kV/cm are 20, 28, and 17 for the superlattices with 10, 16, and 20 nm individual layer thickness, respectively, compared to 10 for single layer $BaTiO_3$ thin film of equal thickness. It is clear from the figure that the superlattice exhibits better dielectric properties than the homogeneous single layer thin film of the constituent materials. The relatively higher tunability (~55%) and figure of merit obtained around 300 K

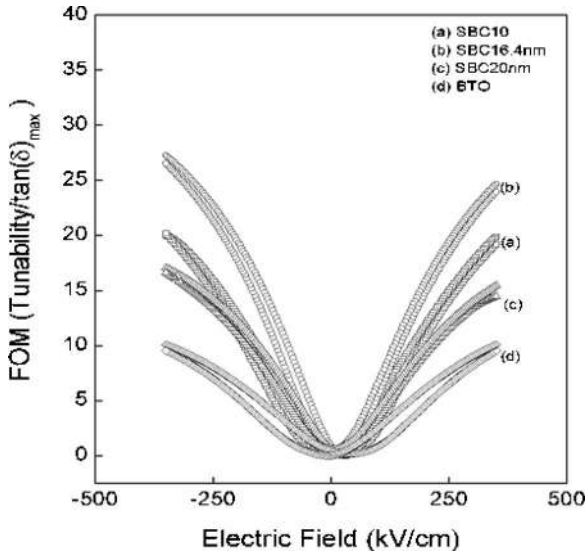

FIG. 6. Figure of merit (FOM) of SBC superlattice thin films as a function of electric field for different individual layer thickness. (a) 10 nm, (b) 16.4 nm, (c) 20 nm, (d) single layer BTO with the same total thickness.

indicates that the superlattice is a potential electrically tunable material for microwave devices at room temperature.

IV. CONCLUSIONS

In summary, SBC superlattices with varying individual layer thicknesses were fabricated using pulsed laser ablation technique on platinized silicon substrates. The presence of satellite reflections in XRD analysis and a periodic concentration of Sr, Ba, and Ca throughout the film in-depth profile of SIMS analysis confirm the fabrication of superlattice structures. The polarization studies show a clear size dependent polarization behavior of the superlattices. On increasing interlayer thickness, the saturation (P_s) and remnant (P_r) polarization increases gradually, reaches a maximum at a certain thickness, and then decreases. The *C-V* curves also exhibit clear thickness dependence. The tunability of these structures was around 55% and was found to be higher than any of the single homogeneous polycrystalline thin film of the constituent materials. The decrease in polarization on increase of periodicity could be attributed to the reduced interfacial strain and tends to behave as individual systems put together. The interfacial strain giving rise to a strained polar region due to high lattice mismatch and electrostatic coupling due to polarization mismatch between the layers account for the enhanced properties.

[1]H. N. Lee, H. M. Christen, M. F. Chisholm, C. M. Rouleau, and D. H. Lowndes, Nature (London) **433**, 395 (2005).
[2]M. P. Warusawithana, E. V. Colla, J. N. Eckstein, and M. B. Weissman, Phys. Rev. Lett. **90**, 036802 (2003).
[3]N. Sai, B. Meyer, and D. Vanderbilt, Phys. Rev. Lett. **84**, 5636 (2000).
[4]J. B. Neaton and K. M. Rabe, Appl. Phys. Lett. **82**, 1586 (2003).
[5]S. M. Nakhmanson, K. M. Rabe, and D. Vanderbilt, Appl. Phys. Lett. **87**, 102906 (2005).
[6]L. Kim, D. Jang, J. Kim, Y. S. Kim, and J. Lee, Appl. Phys. Lett. **82**, 2118 (2003).
[7]C. H. Ahn, K. M. Rabe, and J. M. Triscone, Science **303**, 488 (2004).
[8]J. M. Gregg, J. Phys.: Condens. Matter **15**, V11 (2003).
[9]G. Rijnders and D. H. A. Blank, Nature (London) **433**, 369 (2005).
[10]J. Shen and Y.-q. Ma, Phys. Rev. B **61**, 14279 (2000).
[11]B. D. Qu, W. L. Zong, and R. H. Prince, Phys. Rev. B **55**, 11218 (1997).
[12]J. Shen and Y.-q. Ma, J. Appl. Phys. **89**, 5031 (2001).
[13]R. Ranjith, R. Nikhil, and S. B. Krupanidhi, Phys. Rev. B **74**, 184104 (2006).
[14]A. Sarkar and S. B. Krupanidhi, J. Appl. Phys. **101**, 104113 (2007).
[15]J. Junquera and P. Ghosez, Nature (London) **422**, 506 (2003).
[16]M. Dawber, C. Lichtensteger, M. Cantoni, M. Veithen, P. Ghosez, K. Johnston, K. M. Rabe, and J. M. Triscone, Phys. Rev. Lett. **95**, 177601 (2005).
[17]M. Sepliarsky, S. R. Phillpot, D. Wolf, M. G. Stachiotti, and R. L. Migoni, Phys. Rev. B **64**, 060101 (2001).
[18]S. Zhong, S. P. Alpay, and J. V. Mantese, Appl. Phys. Lett. **87**, 102902 (2005).
[19]A. L. Roytburd, S. Zhong, and S. P. Alpay, Appl. Phys. Lett. **87**, 092902 (2005).
[20]S. Zhong, S. P. Alpay, and J. V. Mantese, Appl. Phys. Lett. **88**, 132904 (2006).
[21]F. De Flaviis, N. G. Alexopoulos, and M. Staffsudd, IEEE Trans. Microwave Theory Tech. **45**, 963 (1997).
[22]V. K. Varadan, D. K. Ghodgaonker, V. V. Varadan, J. F. Kelly, and P. Glikerdas, Microwave J. **35**, 116 (1992).
[23]M. Shen, S. Ge, and W. Cao, J. Phys. D **34**, 2935 (2001).
[24]Armin Segmuller and A. E. Blakeslee, J. Appl. Crystallogr. **6**, 19 (1973).
[25]O. I. Lebedev, J. F. Hamet, G. Van Tendeloo, V. Beaumont, and B. Raveau, J. Appl. Phys. **90**, 5261 (2001).
[26]V. A. Stephanovich, I. A. Lukyanchuk, and M. G. Karkut, Phys. Rev. Lett. **94**, 047601 (2005).
[27]Y. Z. Wu, P. L. Yu, and Z. Y. Li, J. Appl. Phys. **91**, 1482 (2002).
[28]H. Diamond, J. Appl. Phys. **32**, 909 (1961).
[29]V. Ya. Shur and E. L. Rumyantsev, Ferroelectrics **191**, 319 (1997).
[30]S. B. Krupanidhi and D. Roy, Integr. Ferroelectr. **1**, 253 (1992).
[31]S. G. Lu, X. H. Zhu, C. L. Mak, K. H. Wong, H. L. W. Chan, and C. L. Choy, Appl. Phys. Lett. **82**, 2877 (2003).